Nonlinear Site Amplification as Function of 30 m Shear Wave Velocity

Yoojoong Choi,[a] M.EERI, and Jonathan P. Stewart,[b] M.EERI

We develop empirical relationships to predict nonlinear (i.e., amplitude-dependant) amplification factors for 5% damped response spectral acceleration as a continuous function of average shear wave velocity in the upper 30 m, $V_{s\text{-}30}$. We evaluate amplification factors as residuals between spectral accelerations from recordings and modified rock attenuation relationships for active regions. Amplification at low- and mid-periods is shown to increase with decreasing $V_{s\text{-}30}$ and to exhibit nonlinearity that is dependent on $V_{s\text{-}30}$. The degree of nonlinearity is large for NEHRP Category E ($V_{s\text{-}30}<180$ m/s) but decreases rapidly with $V_{s\text{-}30}$, and is small for $V_{s\text{-}30}>\sim 300$ m/s. The results can be used as $V_{s\text{-}30}$-based site factors with attenuation relationships. The results also provide an independent check of site factors published in the *NEHRP Provisions*, and apparent bias in some of the existing NEHRP factors is identified. Moreover, the results provide evidence that data dispersion is dependent on $V_{s\text{-}30}$.
[DOI: 10.1193/1.1856535]

INTRODUCTION

Most modern U.S. seismic design codes for building structures represent seismic demand in terms of 5%-damped response spectral ordinates. These spectral ordinates are affected by seismic source, travel path, and site response effects. In the *NEHRP Recommended Provisions for Seismic Regulations for New Buildings and Other Structures, Part 1: Provisions* and *Part 2: Commentary* (BSSC 2001), source and path effects are accounted for in maps showing the results of probabilistic seismic hazard analyses (PSHA) for the United States (Frankel et al. 2000) and so-called maximum considered earthquake (MCE) maps, which are modified from PSHA maps using deterministic seismic hazard analyses (DSHA) in areas of large hazard by consensus judgment (Leyendecker et al. 2000). These maps are prepared for a particular site condition referred to as the reference site condition. In the *NEHRP Provisions*, site condition is generally parameterized on the basis of the average shear wave velocity in the upper 30 m of the site ($V_{s\text{-}30}$), which is defined as the ratio of 30 m to the vertical shear-wave travel time through the upper 30 m of the site. The $V_{s\text{-}30}$-based site categories in the *NEHRP Provisions* are given in Table 1. An exception to the $V_{s\text{-}30}$ criteria is made for soft clays (defined as having undrained shear strength <24 kPa, plasticity index >20, and water con-

[a] Staff Engineer, GeoPentech, 601 N. Parkcenter Drive, #210, Santa Ana, CA 92705
[b] Associate Professor, Civil & Environmental Engineering Dept., University of California, Los Angeles, CA 90095

Table 1. Site categories in *NEHRP Provisions* (Martin 1994)

NEHRP Category	Description	Mean Shear Wave Velocity to 30 m
A	Hard rock	>1500 m/s
B	Firm to hard rock	760–1500 m/s
C	Dense soil, soft rock	360–760 m/s
D	Stiff soil	180–360 m/s
E	Soft clays	<180 m/s
F	Special study soils, e.g., liquefiable soils, sensitive clays, organic soils, soft clays >36 m thick	

tent >40%), for which category E is assigned if the thickness of soft clay exceeds 3 m regardless of $V_{s\text{-}30}$. The reference site condition for which the PSHA maps are intended to apply is the B-C boundary, or $V_{s\text{-}30}$=760 m/s.

The effects on spectral ordinates of site conditions that deviate from the reference velocity are accounted for with site factors that are a function of site category and the amplitude of shaking for the reference site condition (Dobry et al. 2000). The site factors given in the *NEHRP Provisions* are plotted in Figure 1. By definition, site factors represent the ratio of spectral ordinates for a particular site condition to the value of the ordinates that would be expected for the reference condition. The specific factors given in the provisions are F_a, which is defined over a low-period range (T=0.1–0.5 s), and F_v, which is defined over a mid-period range (T=0.4–2.0 s). The ground motion parameters for the reference site condition that are used in conjunction with site factors are T=0.2 s spectral acceleration (S_a) for F_a (denoted S_s) and S_a at T=1.0 s for F_v (denoted S_1). When the design ground motions are estimated as the product of the amplification factors given in Figure 1 and spectral ordinates S_s or S_1 derived from PSHA, two implicit assumptions are being made: (1) the amplification factor defines the ratio of the median ground motion amplitude on the subject site condition to the median amplitude on the reference site condition, and (2) the data dispersion within the two site categories is

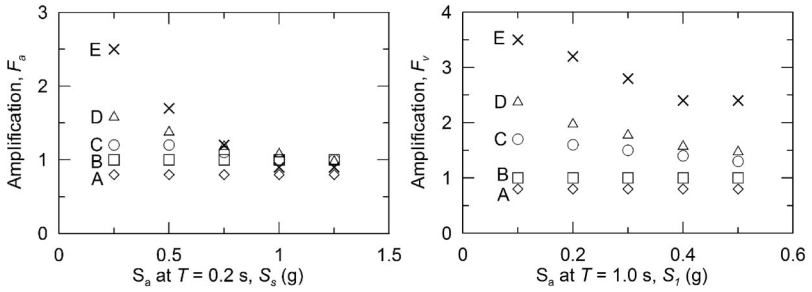

Figure 1. Site factors F_a and F_v given in the *NEHRP Provisions* (BSSC 2001).

identical. The former assumption is correct as long as both distributions are lognormally distributed, while the accuracy of the second assumption is investigated subsequently in the paper.

One important element of PSHA or DSHA is the attenuation relationship used to evaluate the probabilistic distribution of a given spectral ordinate given that an earthquake with particular source characteristics (e.g., moment magnitude, focal mechanism) has occurred at a particular distance from the site. The output of an attenuation model applies only for a particular site condition (i.e., the average site condition at the strong motion accelerometers that produced the data used to derive the attenuation relation), and hence PSHA/DSHA results also apply only for the average site condition in the attenuation model. It follows from the above that since the B-C boundary is the reference condition that the NEHRP PSHA and MCE maps are intended to apply for, the attenuation relations used in the hazard analyses should also be appropriate for this site condition. Unfortunately, this is not the case. The attenuation relations used to develop the PSHA maps for $T>0$ s spectral ordinates (i.e., not peak acceleration) in the 2000 version of the *NEHRP Provisions* are Boore et al. (1997) and Sadigh et al. (1997). The Boore et al. relation can be implemented directly for the B-C boundary because site condition is parameterized by $V_{s\text{-}30}$. However, the ground motions used to define the rock attenuation model by Sadigh et al. were recorded primarily at rock and shallow ($<$20 m) soil sites in California, most of which have $V_{s\text{-}30}$ values significantly less than 760 m/s. In fact, a borehole compilation by Silva et al. (1997) for this particular "rock" site condition found the median value of $V_{s\text{-}30}$ to be approximately 520 m/s. A similar compilation by Boore et al. (1997) found an average velocity for rock sites of about 620 m/s.

Given the above, the fact that the NEHRP PSHA and MCE maps were derived with these relations (with equal weight given to each) suggests that the actual reference site condition is not the assumed value of 760 m/s, but actually corresponds to a softer condition. The hazard analyses underlying the 2003 maps were expanded to include the Abrahamson and Silva (1997) and Campbell and Bozorgnia (2003) attenuation relations, although these relations were also developed for site categories inconsistent with the NEHRP B-C boundary.

In this paper, we develop statistical models for site factors that are a function of $V_{s\text{-}30}$ and the amplitude of shaking on the reference site condition. The models are developed from statistical analyses of residuals between recorded ground motions in active regions and reference motion predictions developed using modified rock attenuation relationships. The models are useful as follows:

1. to validate the existing NEHRP site factors (which were developed based on both observation and analysis, as discussed further below);
2. as site terms for use with attenuation relations;
3. to identify variations in data dispersion with magnitude, distance, and $V_{s\text{-}30}$; and
4. to develop correction factors that can be used to adjust the predictions of at-

tenuation models (i.e., Abrahamson and Silva 1997, Campbell and Bozorgnia 2003, Sadigh et al. 1997) to the NEHRP-assumed reference condition ($V_{s\text{-}30}$=760 m/s).

The third item above is important because the NEHRP PSHA maps are based on the dispersion estimated from attenuation relations (which is generally independent of site condition). Values of dispersion for specific site conditions that depart significantly from those in the attenuation relations would imply that the mapped PSHA spectral ordinates are biased for those site conditions. The fourth item above is important for the development of PSHA maps applicable to the NEHRP B-C site condition. Application of correction factors has been discussed in past committee deliberations, but has not yet been carried out for the Abrahamson and Silva, and Sadigh et al. attenuation functions (the Campbell and Bozorgnia results were corrected using the linear site factor model of Boore et al. 1997; K. Campbell 2003 pers. comm.).

EXISTING NEHRP AMPLIFICATION FACTORS

The NEHRP site factors shown in Figure 1 are based on both empirical data analysis and the results of ground response analyses (Dobry et al., 2000). The empirical studies were performed by Borcherdt and Glassmoyer (1994), Borcherdt (1994), and Joyner et al. (1994) using strong motion data recorded in the San Francisco Bay Area during the 1989 Loma Prieta earthquake, and provide amplification factors (F_a and F_v) that apply for relatively weak levels of shaking (peak horizontal acceleration for reference [rock] site condition, $PHA_r \approx 0.1$ g). These amplification factors were derived using a so-called reference site approach, in which the amplification is defined as the ratio of Fourier spectral ordinates of motions recorded on soil to those recorded on nearby reference rock sites, with appropriate corrections for variations in site-source distance between the two accelerometers. The analytical studies consisted of one-dimensional equivalent linear and nonlinear ground response analyses by Dobry et al. (1994) and Seed et al. (1994), and were used to extend the F_a and F_v values to $PHA_r \approx 0.4–0.5$ g. For both the empirical and analytical studies, site factors were defined relative to a competent rock site condition, which in the San Francisco Bay Area corresponds specifically to Franciscan formation bedrock of Cretaceous and Jurassic age.

Since the adoption of the site factors in Figure 1, a number of studies have investigated the adequacy of the NEHRP factors by comparing them to alternative factors derived using non–Loma Prieta strong motion data sets (e.g., from Northridge recordings [Borcherdt 2002a, b], numerous southern California earthquakes [Harmsen 1997, Field 2000, Steidl 2000], and strong motion databases for active regions [Joyner and Boore 2000, Stewart et al. 2003]). Work has also been performed using alternative site categorization schemes (Rodriguez-Marek et al. 2001, Stewart et al. 2003), although this is not discussed here as the present focus is on $V_{s\text{-}30}$-based site categories.

Borcherdt (2002a, b) investigated amplification levels within NEHRP categories using recordings from the 1994 Northridge earthquake, mostly from stiff soil and soft rock sites. A reference site approach was used to define amplification factors, with reference motions taken from local stations with metamorphic rock (e.g., weathered granite,

gneiss) or sedimentary rock (in which case amplification factors were adjusted so that the effective reference site condition is relatively firm rock). Average Northridge amplification factors were found to match very well with the NEHRP amplification factors at both small periods (F_a) and at longer periods (F_v). The Northridge results also demonstrated decreasing amplification with increasing reference motion amplitude, an effect that had not been observed from the Loma Prieta recordings. This effect was not observed in Loma Prieta because most recordings sites are at large distances from the source, so that PHA_r values were small.

The work by Harmsen (1997) involved the evaluation of amplification factors within NEHRP categories using data from multiple southern California earthquakes normalized relative to a single reference rock site (Caltech Seismic Lab). A number of researchers affiliated with the Southern California Earthquake Center (SCEC) evaluated amplification factors using a consistent data set consisting only of southern California earthquakes (Field 2000, Steidl 2000). Field (2000) evaluated amplification factors as a direct function of $V_{s\text{-}30}$ using a non-reference site approach in which amplification factors were derived as a term within a southern California attenuation relationship. Steidl (2000) also used a non-reference site approach, evaluating site factors as a function of $V_{s\text{-}30}$ using residuals from the Sadigh et al. (1993) attenuation relationship for rock sites (similar to the Sadigh et al. 1997 relation). The amplification factors from the Harmsen and Field studies are independent of PHA_r. In the Steidl study, amplification factors were developed for $PHA_r < 0.1$ g and all PHA_r ranges.

Joyner and Boore (2000) developed amplification factors within NEHRP categories using a procedure similar to that of Field (2000) described above, although the short period factors are expressed as a function of reference motion amplitude. Stewart et al. (2003) developed nonlinear amplification factors within NEHRP categories relative to the Abrahamson and Silva (1997) attenuation relationship.

Most of the above models provide discrete amplification factors within NEHRP categories; only the Field and Harmsen studies provide amplification factors as a continuous function of $V_{s\text{-}30}$. At present, there are no amplification models that are both PHA_r-dependent and a continuous function of $V_{s\text{-}30}$. Amplification factors from the above studies are compared to each other and to the results of this study subsequently in this paper (Figure 10).

DATA RESOURCES

STRONG MOTION DATA

The ground motion database used in this study consists of 1828 recordings from 154 earthquakes. These recordings are from worldwide shallow crustal earthquakes near active plate margins. Subduction and interplate events are excluded. Event dates range from the 1933 Long Beach, California, earthquake to the 1999 Duzce, Turkey, earthquake. Removed from the data set for this study were recordings from events with poorly defined magnitude or focal mechanism, recordings for which site-source distances are poorly constrained, recordings at large distance (>100 km), and recordings for which problems were detected with one or more components. The recordings at large

distance were eliminated because the currently available data is too sparse to support the development of empirical ground motion models at that distance range. These removals reduced the data set to 919 recordings from 59 events. Data from the 1999 Chi-Chi, Taiwan, earthquake were not used in this study due to the preliminary nature of the site classifications. Additional information on characteristics of the strong motion data set is provided by Stewart et al. (2001).

The sources of strong motion data for the western United States include the California Strong Motion Instrumentation Program (CSMIP), the U.S. Geological Survey (USGS), the University of Southern California (USC), the California Division of Mines and Geology (CDMG), and the Los Angeles Department of Water and Power (LADWP). Additional data have been obtained for the 1999 Kocaeli and Duzce, Turkey, earthquakes from the Kandilli Observatory and Earthquake Engineering Research Institute of Boçizi University (Kandilli), the Earthquake Research Department of the General Directorate of Disaster Affairs (ERD), and Istanbul Technical University (ITU). Most of the time histories used in this study can be obtained at the web site of the Pacific Earthquake Engineering Research Center (www.peer.berkeley.edu).

DATA USED FOR SITE CLASSIFICATIONS

In order to classify strong motion sites according to the $V_{s\text{-}30}$ parameter, a GIS database was developed having the locations of both strong motion stations and boreholes in California. Each strong-motion station location was checked with instrument owners (USGS and CSMIP), or against published reports (Anderson et al., 1981), to optimize accuracy. Borehole locations were generally obtained from maps in reports. The borehole database is similar to that of Wills and Silva (1998), but also contains additional Caltrans boreholes, boreholes from selected consulting geotechnical engineers, and data recently compiled in the ROSRINE program (http://geoinfo.usc.edu/rosrine/). These databases were used to match boreholes with strong motion sites if (1) both locations are on the same surface geology and (2) the separation distance was $<$1600 m.

The above databases were used to pair 209 strong motion stations to boreholes with geophysical measurements. Of these sites, 174 have borehole-accelerograph separation distances less than 160 m, 13 from 160 to 450 m, and 22 from 450 to 1600 m. The borehole geophysical data was used to develop $V_{s\text{-}30}$ values for the paired strong motion stations. Sites were classified into NEHRP categories on the basis of these $V_{s\text{-}30}$ values, although a site was classified as E if $V_{s\text{-}30} \leqslant 180$ m/s or if the thickness of soft clay (defined above) is greater than 3 m. The distribution of $V_{s\text{-}30}$ values for sites in our database is shown in Figure 2 along with the median $V_{s\text{-}30}$ value in each well-populated category. It should be noted that shear wave velocities for USC strong motion stations obtained by Rodriguez-Ordonez (1994) were not used due to apparent biases in such data as documented by Boore and Brown (1998) and Wills and Silva (1998). A complete inventory of the classifications is presented in Stewart et al. (2001).

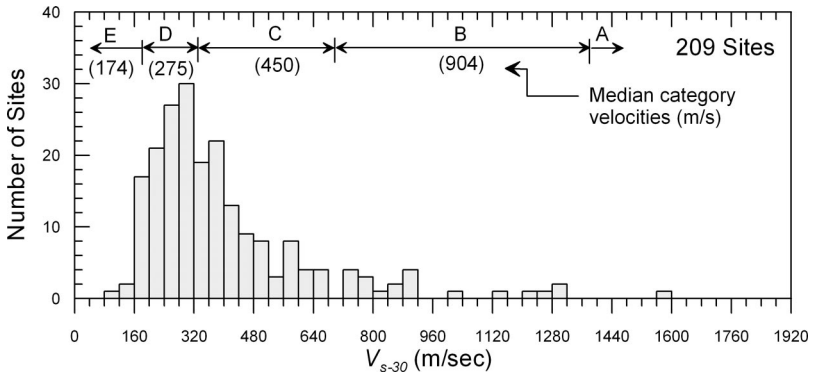

Figure 2. Histogram of $V_{s\text{-}30}$ values for strong motion sites used in this study.

DEVELOPMENT OF AMPLIFICATION MODEL

Model development begins with two stages of preliminary analysis. In the first stage, amplification factors within bins defined on the basis of $V_{s\text{-}30}$ are investigated to evaluate the variation of nonlinearity (i.e., dependence of amplification on PHA_r) with $V_{s\text{-}30}$. In the second stage, amplification levels near a baseline reference amplitude of $PHA_r = 0.1$ g are studied to identify an appropriate model for the variation of amplification (at the baseline amplitude) with $V_{s\text{-}30}$. The baseline amplitude of 0.1 g was selected because it represents a mid-range amplitude on a log-scale for motions in most site categories. Results from these two stages of analysis are used to develop a functional form for a "unified" model (i.e., a model that combines the effects of $V_{s\text{-}30}$ and nonlinearity). The regression parameters for this unified model are then evaluated using a mixed-effects regression procedure (e.g., Abrahamson and Youngs 1992). The following subsections describe the two stages of preliminary data analysis, the regression analyses used to develop the unified model, comparisons of model predictions to data, and the analysis of standard deviation terms.

AMPLIFICATION WITHIN $V_{S\text{-}30}$ CATEGORIES

Amplification factors within $V_{s\text{-}30}$ categories are compiled to evaluate the degree to which nonlinearity in amplification factors varies with $V_{s\text{-}30}$. These data analysis procedures are similar to those of Stewart et al. (2003), and hence are reviewed only briefly.

The amplification factor for ground motion j within site category i, F_{ij}, is evaluated in arithmetic units from the geometric mean of 5% damped acceleration response spectra for the two horizontal components of shaking, S_{ij}, and the reference ground motion for the site, $(S_r)_{ij}$, as follows:

$$F_{ij}(T) = S_{ij} / (S_r)_{ij}, \tag{1}$$

where T=spectral period. In Equation 1, S_{ij} and $(S_r)_{ij}$ are computed at the same spectral period, which is varied from 0.01 to 5.0 s. Amplification factors are not evaluated for $T>1/(1.25\times f_{hp})$, where f_{hp}=high-pass corner frequency.

For the preliminary analyses discussed in this subsection, reference motion parameter $(S_r)_{ij}$ is taken as the median spectral acceleration calculated from the Abrahamson and Silva (1997) A&S attenuation relationship for rock sites, with modifications for rupture directivity effects and event terms. The A&S rock attenuation relationship provides ground motion estimates that are appropriate for a soft rock site condition with $V_{s\text{-}30}$ values reported to be in the range of 520 to 620 m/s (Silva et al. 1997, Boore et al. 1997). The rupture directivity correction is made for sites near the seismic source using the empirical model by Somerville et al. (1997), later modified by Abrahamson (2000). For well-recorded events, the event term represents the period-dependent average residual between motions from a given event and the general attenuation model (the event terms used at this stage of the analyses were provided by Abrahamson [1999, pers. comm.]). These terms are evaluated during the development of attenuation models with a mixed-effects regression procedure (Abrahamson and Youngs 1992). The use of an event term in the evaluation of $(S_r)_{ij}$ is intended to remove bias in the attenuation model that might be present for a particular event.

Amplification factors computed using Equation 1 were sorted into the following $V_{s\text{-}30}$ categories for intracategory regression analysis:

E: $V_{s\text{-}30}<180$ m/s+soft clay

D_{lv}: $180<V_{s\text{-}30}<310$ m/s

CD: $310<V_{s\text{-}30}<520$ m/s

C_{hv}: $520<V_{s\text{-}30}<760$ m/s

B: $760<V_{s\text{-}30}<1500$ m/s

These ranges of $V_{s\text{-}30}$ essentially match the NEHRP categories, except that NEHRP C and D are subdivided into three bins (C_{hv}, CD, and D_{lv}) to better capture the variation of site nonlinearity with $V_{s\text{-}30}$. Within category i, regression analyses were performed to relate amplification factors, F_{ij}, to ground motion amplitude as follows:

$$\ln(F_{ij})=a_i+b_i\ln(G_{ij})+\varepsilon_{ij}, \tag{2}$$

where a_i and b_i are regression coefficients specific to category i, G_{ij} is a parameter representing the amplitude of the reference ground motion for site j, and ε_{ij} is an error term (i.e., ε_{ij} is the residual between data and model). This same regression equation has been used by Youngs (1993), Bazzuro (1998), and Stewart et al. (2003), with G_{ij} taken as PHA_r. We also take G_{ij} as PHA_r.

Using the data within the above velocity ranges, regression analyses were performed according to Equation 2 using ordinary least-squares procedures in which equal weight is given to all data points. The least-squares procedure is used because of the inclusion

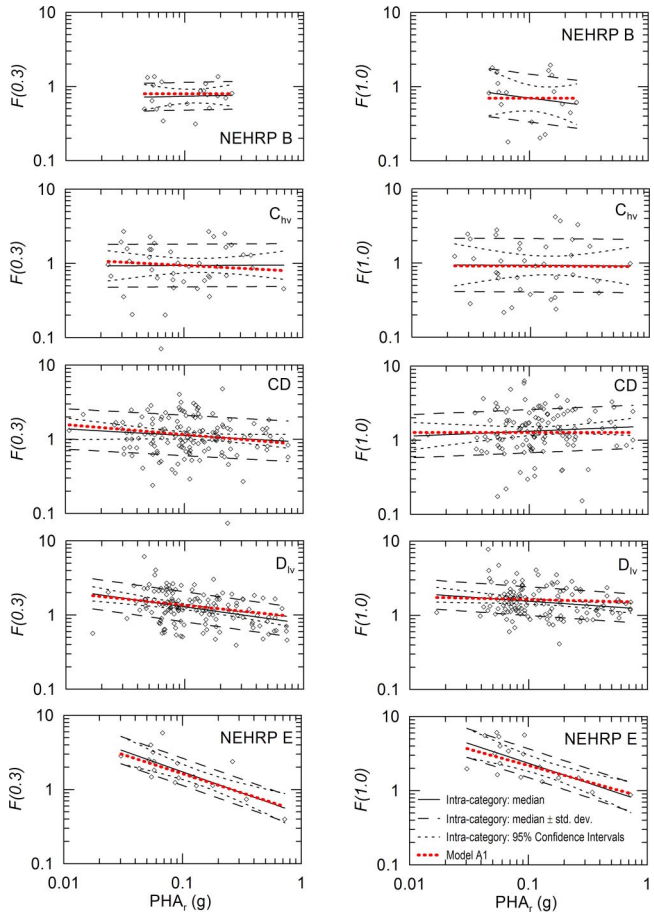

Figure 3. Spectral acceleration amplification factors, intracategory regression results, and predictions of unified model for velocity categories plotted relative to PHA of reference motion (PHA_r).

of event terms in $(S_r)_{ij}$. For each $V_{s\text{-}30}$ category, we plot in Figure 3 spectral amplification levels for the periods of $T=0.3$ s [$F(0.3)$] and $T=1.0$ s [$F(1.0)$]. Also plotted are results of regression analyses performed according to Equation 2 (solid lines), ±95% confidence intervals on the median amplification (dotted lines), and median regression ±lognormal standard deviation term (dashed lines). Note that the thick dotted lines in Figure 3 represent predictions of the unified model that are discussed subsequently in the paper. Presented in Table 2 are regression coefficients and standard deviation terms for the ground motion parameters of $F(0.3)$ and $F(1.0)$. The estimation error terms for parameters a_i and b_i in Table 2 are the half-widths of the ±95% confidence intervals on the parameters.

Reductions of amplification factors with increasing reference motion amplitude are taken as evidence of sediment nonlinearity. This nonlinearity is quantified

Table 2. Regression coefficients for S_a amplification factors

Category	Period	a	b	Std. Dev.	Rejection confidence for b=0 model (%)
B	0.3	−0.23±0.88	0.03±0.37	0.44	14
	1.0	−0.84±1.63	−0.21±0.68	0.77	48
C_{hr}	0.3	−0.05±0.64	0.01±0.26	0.67	4
	1.0	−0.09±0.85	−0.01±0.35	0.84	5
CD	0.3	−0.09±0.30	−0.09±0.13	0.63	83
	1.0	0.43±0.37	0.07±0.16	0.67	58
D_{lr}	0.3	−0.26±0.22	−0.23±0.10	0.47	100
	1.0	0.19±0.22	−0.11±0.10	0.45	97
E	0.3	−0.76±0.69	−0.57±0.28	0.44	100
	1.0	−0.37±0.73	−0.53±0.29	0.46	100

by the b_i parameter for each category i. The statistical significance of the nonlinearity is assessed two ways. The first significance test consists of comparing the absolute value of b_i to the estimation error for b_i (both indicated in Table 2). When $|b_i|$ exceeds the estimation error, the nonlinearity is considered significant. Secondly, sample "t" statistics are compiled to test the null hypothesis that $b_i=0$ and $a_i=$overall data median. This statistical testing provides a significance level$=\alpha$ that the null hypothesis cannot be rejected. For clarity of expression, we tabulate in Table 2 values of $1-\alpha$, which we refer to as a "rejection confidence for a $b=0$ model." Large rejection confidence levels (i.e., greater than 95%) suggest significant PHA_r-dependence in amplification factors.

The b parameters compiled from the above analyses are plotted as discrete data points with error bounds in Figure 4. The results show statistically significant nonlinearity (by the above criteria) at small $V_{s\text{-}30}$, corresponding to the E category. Values of b decrease to a relatively consistent value slightly offset from zero for $V_{s\text{-}30}>\sim 300$ m/s. The nonlinearity at these large $V_{s\text{-}30}$ values is not statistically significant. Based on the trend of the discrete points in Figure 4, we postulate the following model to simulate the variation of b with PHA_r:

$$b=b_1 \qquad \text{Category E} \tag{3a}$$

$$b=b_2+(V_{s\text{-}30}-b_V)^2\frac{b_1-b_2}{(180-b_V)^2} \qquad 180<V_{s\text{-}30}<b_V \text{ (m/s)} \tag{3b}$$

$$b=b_2 \qquad b_V<V_{s\text{-}30}<520 \text{ (m/s)} \tag{3c}$$

$$b=b_2-(V_{s\text{-}30}-520)\frac{b_2}{240} \qquad 520<V_{s\text{-}30}<760 \text{ (m/s)} \tag{3d}$$

$$b=0 \qquad V_{s\text{-}30}>760 \text{ (m/s)} \tag{3e}$$

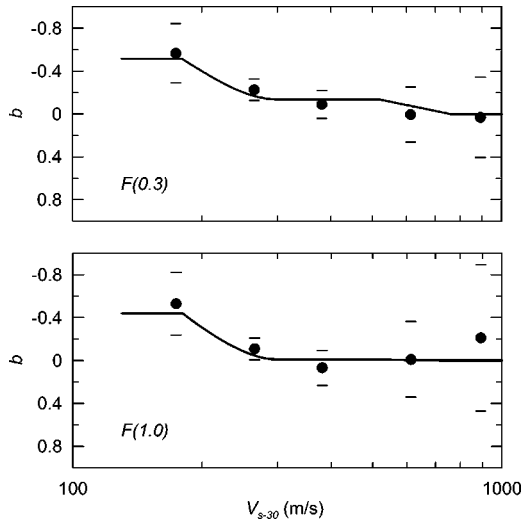

Figure 4. Variation of slope parameter b (defined in Equation 2) with $V_{s\text{-}30}$. Plotted are discrete results for $V_{s\text{-}30}$ data bins and continuous lines showing the model defined by Equation 3, whose parameters are determined from mixed effects regression analyses.

where the units of $V_{s\text{-}30}$ are in m/s, and b_1, b_2, and b_V are model parameters estimated from the data. A parabolic fit for $180 < V_{s\text{-}30} < b_V$ was used in lieu of a linear fit because the parabola predicts lower levels of nonlinearity, which is more consistent with the data. The decrease of b_2 to zero at high $V_{s\text{-}30}$ is motivated by the statistical insignificance of nonlinearity for high velocity sites. Values of parameters b_1, b_2, and b_V were estimated from regression analyses described subsequently in the paper, and the continuous lines in Figure 4 represent the outcome of those analyses.

VARIATION OF AMPLIFICATION WITH $V_{s\text{-}30}$

In this section, we investigate the variation of amplification factors with $V_{s\text{-}30}$, which is accomplished by compiling data points from each category "near" a reference site baseline shaking level of $PHA_r = 0.1$ g. Our use here of only data near this baseline shaking level is intended to isolate the $V_{s\text{-}30}$ dependence of the amplification factors from the dependence on PHA_r.

We identify these data points as follows. Suppose, for example, that the median value of $F(0.3)$ from regression (i.e., Equation 2) at the baseline amplitude is $F^{ba}(0.3)$. We then find the PHA_r values along the median regression fit for the category (i.e., the solid lines in Figure 3) corresponding to an amplification departure (in natural logarithmic units) from $F^{ba}(0.3)$ of 0.05 (i.e., amplification levels in natural logarithmic units of $\ln[F^{ba}(0.3)] \pm 0.05$). Data points between these two PHA_r levels are selected. When the regression fit shows no significant nonlinearity, most or all of the data is selected, whereas significant nonlinearity limits the data range selected (e.g., data was taken only from $PHA_r = 0.09$–0.11 g for $F^{ba}(0.3)$ s in NEHRP Category E). The value of ± 0.05

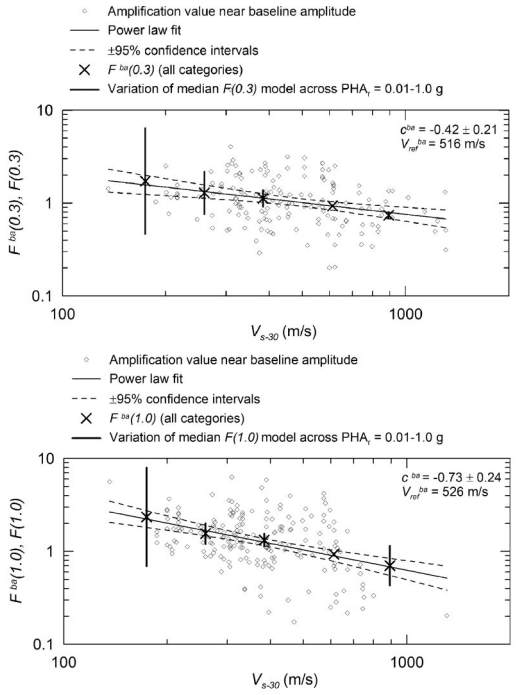

Figure 5. Variation of amplification factors $F^{ba}(0.3)$ and $F^{ba}(1.0)$ with $V_{s\text{-}30}$ for consistent ground motion amplitude (data points and power law regression fit), along with intracategory variation of $F(0.3)$ and $F(1.0)$ with reference motion amplitude (vertical lines).

used in the above process was selected by judgment; it was found to provide a collection of data points that is sufficiently large that statistically stable amplification values can be defined while simultaneously maintaining insignificant PHA_r—dependence of amplification.

Data points selected by the above process are shown in Figure 5 along with a regression fit using the following power law equation:

$$F^{ba}(T)=\left(\frac{V_{s\text{-}30}}{V_{ref}^{ba}}\right)^{c^{ba}} \tag{4}$$

where V_{ref}^{ba} and c^{ba} are regression coefficients (given in Figure 5) and superscript "ba" on $F(T)$ and the regression parameters denotes the use of amplification factors selected by the above process (i.e., near the baseline amplitude). Note that parameter V_{ref}^{ba} is simply the value of $V_{s\text{-}30}$ at which $F^{ba}(T)$ is unity. Plotted adjacent to the power law fit are the ±95% confidence intervals on the median amplification. Also shown for reference are within-category median $F(0.3)$ and $F(1.0)$ values at PHA_r=0.1 g (i.e., the ordinates of the solid lines from Figure 3 at PHA_r=0.1 g), which are plotted with an × at the median $V_{s\text{-}30}$ value for within-category data. The vertical line drawn through the × represents the

range of amplification values that would be expected for PHA_r=0.01–1.0 g based on intracategory regression results. The results in Figure 5 show the expected significant increase of amplification with decreasing $V_{s\text{-}30}$, although the variation with reference motion amplitude is also important (especially for Category E).

MIXED-EFFECTS REGRESSION FOR UNIFIED MODEL

The models for $V_{s\text{-}30}$- and PHA_r-dependence of amplification in Equations 3 and 4 can now be combined to form a unified model for amplification factors. This model is expressed as follows:

$$\ln(F_{ij}) = c \ln\left(\frac{V_{s\text{-}30_{ij}}}{V_{ref}}\right) + b \ln\left(\frac{PHA_{r_{ij}}}{0.1}\right) + \eta_i + \varepsilon_{ij}, \quad (5)$$

where PHA_r is expressed in units of g; b is a function of regression parameters as given in Equation 3; c and V_{ref} are regression parameters; η_i is a random effect term for earthquake event i (should have zero median across all events, standard deviation is denoted as τ); and ε_{ij} represents the intra-event model residual for motion j in event i (should have median near zero for well-recorded events, standard deviation is denoted σ). In order to simplify the regression process to produce stable results, parameter b_2 in Equation 3 was estimated using all data with $V_{s\text{-}30} > b_V$. However, as a practical matter, the data controlling b_2 in the regression are sites with velocities between approximately 300 and 600 m/s. As noted previously, the decrease of b_2 to zero at high $V_{s\text{-}30}$ is a judgment-based adjustment to the model motivated by the statistical insignificance of nonlinearity for high velocity sites.

The total standard deviation that is appropriate for use with the median amplification from Equation 5 is

$$\sigma_{total} = \sqrt{\sigma^2 + \tau^2} \quad (6)$$

We perform regression analyses according to Equation 5 using a mixed-effects procedure similar to Abrahamson and Youngs (1992) as implemented in the program R (Pinheiro and Bates 2000). The amplification factors used in these regressions are modified from those presented above (i.e., Equation 1), in that event terms are not incorporated into the reference site ground motions, S_r. We omit event terms from the reference motion at this stage because event terms are estimated as part of the mixed-effects regression procedure (i.e., term η_i). In addition, reference motions are now evaluated using multiple attenuation models. The models and corresponding site conditions used to evaluate S_r values are as follows:

A1. Abrahamson and Silva (1997) A&S: rock

A2. Sadigh et al. (1997): rock

A3. Campbell and Bozorgnia (2003) C&B: generic rock

We considered using the Boore et al. (1997) attenuation relationship as well. We chose not to develop site factors relative to this attenuation model in part because the site factor in that attenuation model is already cast in terms of $V_{s\text{-}30}$, with 760 m/s

Table 3. Regression parameters (unsmoothed) for unified model for site amplification. Parameters without error terms are estimated deterministically (as described in text).

Atten. Model	Parameter	b_1	b_2	b_v	c	V_{ref} (m/s)	τ	σ	σ_{total} [1]
A1	*F(0.3)*	−0.41	−0.11±0.05	300	−0.46±0.07	532±93	0.35	0.54	0.64
	F(1.0)	−0.39	0.02±0.05	300	−0.69±0.07	519±69	0.41	0.55	0.69
A2	*F(0.3)*	−0.49	−0.21±0.04	300	−0.44±0.07	601±103	0.29	0.55	0.62
	F(1.0)	−0.48	−0.12±0.05	300	−0.66±0.08	646±90	0.35	0.57	0.67
A3	*F(0.3)*	−0.51	−0.05±0.05	300	−0.44±0.07	610±106	0.29	0.53	0.61
	F(1.0)	−0.49	−0.04±0.06	300	−0.67±0.07	709±107	0.39	0.56	0.68

[1] $\sigma_{total}^2 = \tau^2 + \sigma^2$

taken as the reference value. Moreover, because the strong motion database contains few sites with high $V_{s\text{-}30}$, the Boore et al. attenuation model for the reference site condition is based largely on data from softer sites, and hence the attenuation results are strongly influenced by the (linear) site factor. We felt it was inappropriate to implement an attenuation model that is so dependent on one site factor with a new (different) site factor.

Several issues complicated the regression process. First, a stable estimate of b_V could not be obtained from the regression, so alternative values of b_V were used as fixed values during the regression of other parameters. Optimal b_V values varied somewhat from period to period, but generally a value of 300 m/s provides a reasonable fit to the data. A second complication is that parameter b_1, when estimated by regression, was found to be relatively small in an absolute sense (i.e., indicating small nonlinearity) and to be poorly constrained (i.e., large estimation uncertainty). The low values underpredict the nonlinearity for Category E, for which the available data is not sufficiently abundant to strongly affect the regression results. Accordingly, b_1 was set at values from intracategory regressions.

Example values of model parameters (and their estimation errors) derived directly from the regression are presented in Table 3. The parameters are also listed in the Appendix for $T=0.01-5.0$ s. The results in the Appendix have been smoothed with respect to period.

The c and V_{ref} parameters in Table 3 for Model A1 are similar to those given in Figure 5. As shown by the lines in Figure 4, the parameters describing nonlinearity parameter b for Model A1 define a curve consistent with the b-values from discrete velocity bins.

Median amplification factors for Models A1–A3 are compared in Figure 6 for velocities at the median of the sites within each NEHRP category. The Model A1 and A2 results are generally similar to each other both in terms of the amplification level and the dependence of amplification on PHA_r. At $T=0.3$ s, Model A3 has less PHA_r-dependence for Categories C–D and thus has higher amplification levels for $PHA_r > \sim 0.1$ g. At $T=1.0$ s, A3 amplification levels exceed A1–A2, although the amount of PHA_r-dependence is comparable. For all three models (A1–A3), the

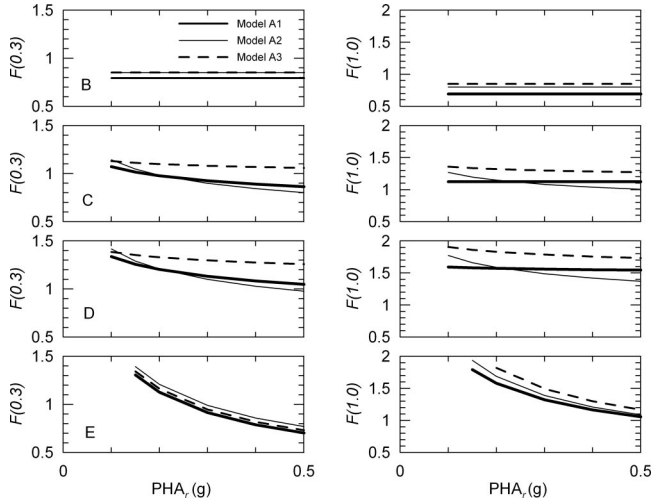

Figure 6. Variation with PHA_r of the median amplification factors from Models A1–A3 at mid-$V_{s\text{-}30}$ value for each NEHRP category.

results are similar for Category E. These differences in the amplification factors for Models A1–A3 result from the different formulations of the respective attenuation models. For example, the relatively linear short-period site terms associated with A3 are a result of different distance-scaling formulations in the attenuation models, which produces relatively low reference rock motions at close distance for C&B (2003) as compared to A&S (1997) or Sadigh et al. (1997). These low reference motions in turn cause the Model A3 amplification factors at close distance (thus high PHA_r) to be large (nearly as high as those at low PHA_r), which results in the minimal nonlinearity.

COMPARISONS OF MODEL PREDICTIONS TO DATA

The sufficiency of the model is investigated by plotting intra-event prediction residuals (ε_{ij} in Equation 5) against $V_{s\text{-}30}$ and PHA_r in Figure 7. Results for Model A1 are shown, although similar results were obtained for Models A2–A3. The results show no apparent trend in model residuals with $V_{s\text{-}30}$ or PHA_r (Figure 7a), and no significant bias for data within the previously used $V_{s\text{-}30}$ bins, as demonstrated by median residuals near unity (Figure 7b). In Figure 3 we plot with thick, dotted lines the model predictions against data within $V_{s\text{-}30}$ bins. The unified model is seen to provide predicted median amplification levels for each category that are reasonably consistent with the intracategory regression results.

ANALYSIS OF STANDARD DEVIATION TERMS

The dispersion of the amplification factors was investigated as a function of magnitude (m), site-source distance (r), and $V_{s\text{-}30}$. The magnitude dependence of dispersion was examined using a procedure similar to that of Youngs et al. (1995).

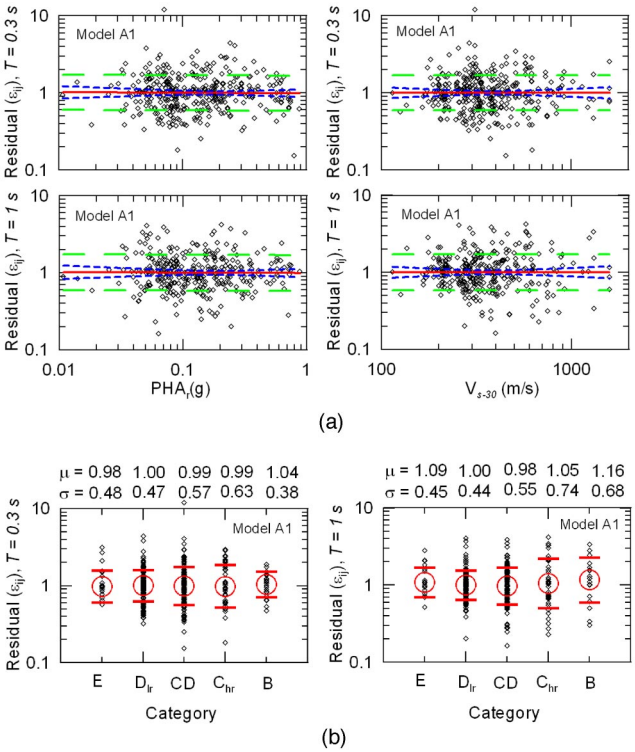

Figure 7. (a) Residuals of Model A1 (in arithmetic units) plotted against $V_{s\text{-}30}$ and PHA_r; and (b) residuals of Model A1 (in arithmetic units) within velocity categories along with the median (μ) and median $\pm$ one standard deviation (σ) of residuals.

The data is binned into groups of 0.5 magnitude width with an overlap of 0.25, and mixed-effects regression analyses are performed within each bin using regression Equation 5, but with the regression coefficients set to the values from the unsmoothed mixed-effect analysis results obtained previously. This analysis provides inter- and intra-event standard deviation terms (τ and σ, respectively) within each magnitude bin. The τ and σ terms and their 95% confidence intervals are plotted in Figure 8a for Model A1 at periods 0.01 s (PHA), 0.3 s, and 1.0 s. Additional analyses (not shown) were performed for Models A2–A3 at the above periods as well as 3.0 s. The confidence intervals on the dispersion reflect the estimation uncertainty, and in general are wide when the data bin is sparsely populated. Note that the confidence intervals around the standard deviation estimates are not symmetric. This is a common feature of variance estimated with a maximum likelihood procedure (Raudenbush and Bryk 2002, p. 55).

The results in Figure 8a do not indicate a significant magnitude-dependence of either τ or σ. Similar results were obtained for Models A2–A3. These results differ from magnitude-dependent standard deviation terms identified by Youngs et al. (1995) and in-

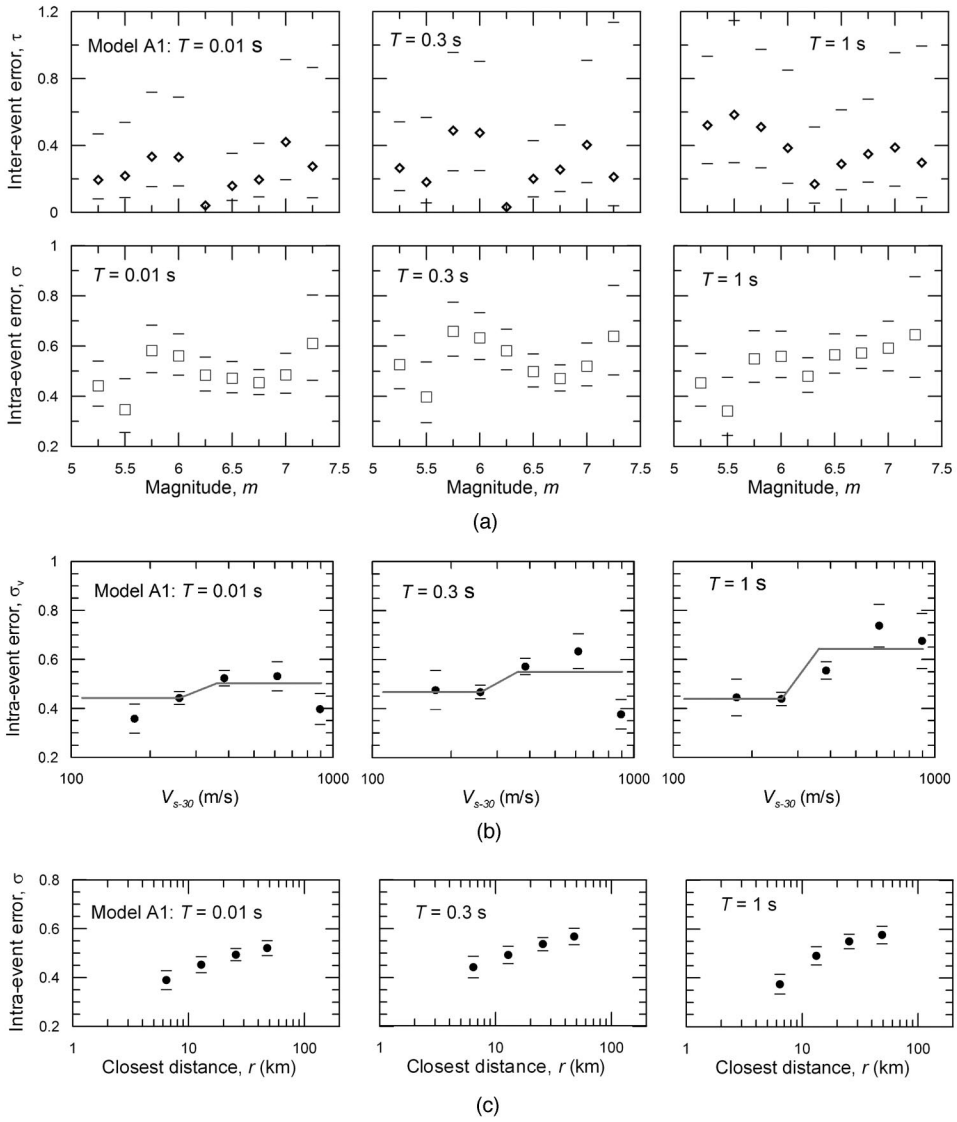

Figure 8. (a) Variation of inter- and intra-event standard deviation (and their estimation error) with magnitude, Model A1; (b) variation of intra-event standard deviation with $V_{s\text{-}30}$, Model A1; and (c) variation of intra-event standard deviation with distance, Model A1.

corporated into most modern attenuation models (e.g., those underlying Models A1–A3). Note also that the confidence intervals on τ are much larger than those on σ. This occurs because there are relatively few earthquakes within each magnitude bin to constrain the τ estimates.

The variation of the dispersion of ε_{ij} (denoted σ) with distance and $V_{s\text{-}30}$ is investigated by partitioning the model residuals according to overlapping distance bins and non-overlapping $V_{s\text{-}30}$ bins, and then evaluating σ within each bin. The results of these analyses are shown in Figure 8b ($V_{s\text{-}30}$) and 8c (distance) for Model A1 at $T=0.01$, 0.3, and 1.0 s. As illustrated in Figure 8b, standard deviation term σ generally increases with $V_{s\text{-}30}$, although the amount of increase is strongly period dependent. At small periods ($T\leqslant\sim0.15$ s) the amount of increase of σ is small between well-populated $V_{s\text{-}30}$ bins for which the results are reliable (generally<0.05). However, for $T\geqslant1.0$ s, the amount of increase between these bins ranges from about 0.1 to 0.3, with larger increases occurring at longer periods. Results for the largest $V_{s\text{-}30}$ bin (760–1300 m/s) vary erratically from period to period due to limited data, and are unreliable.

As shown in Figure 8c, preliminary data analyses indicate that standard deviation terms increase with distance (r) for periods $T\leqslant1.0$ s. However, when the r-dependence of σ is investigated within well-populated $V_{s\text{-}30}$-bins (results not shown for brevity), the trend shown in Figure 8c is lost. Moreover, when the $V_{s\text{-}30}$-dependence of σ is investigated within well-populated r-bins, the trend shown in Figure 8b is retained. Thus, the $V_{s\text{-}30}$-dependence of σ appears to be more significant than the r-dependence.

Based on the above findings, a simple $V_{s\text{-}30}$-dependent model for the intra-event standard deviation is proposed. The standard deviation calculated by this model is denoted σ_v; the symbol σ is retained for the overall intra-event standard deviation without consideration of $V_{s\text{-}30}$. In this model, σ_v is taken as constant at low and high $V_{s\text{-}30}$, with log-linear interpolation for intermediate velocities. The threshold velocities were selected after analysis of many plots similar to those in Figure 8b. The model is cast as follows:

$$\sigma_v=e_1 \qquad V_{s\text{-}30}\leqslant260 \text{ m/s} \tag{7a}$$

$$\sigma_v=e_1+e_2\cdot\ln(V_{s\text{-}30}/260) \qquad 260<V_{s\text{-}30}\leqslant360 \text{ m/s} \tag{7b}$$

where $e_2=(e_3-e_1)/\ln(360/260)$

$$\sigma_v=e_3 \qquad V_{s\text{-}30}>360 \text{ m/s} \tag{7c}$$

An example fit based on Equation 7 is shown by the lines in Figure 8b. Coefficients e_1 and e_3 were evaluated at all periods and are listed in the Appendix. The coefficients were estimated using data from well-populated bins at low and high velocity. The model in Equation 7 necessarily smoothes true bin-to-bin variation of σ, but in general the model is not systematically biased high or low across the suite of periods considered for any particular velocity bin. An exception is soft soil sites (i.e., NEHRP E), for which the model tends to overpredict σ at most periods (although, coincidentally, the model provides a good fit for E at $T=0.3$ and 1.0s, as shown in Figure 8b). For these soft soil sites, standard deviation is better estimated with site-specific ground response analysis (Baturay and Stewart 2003), although use of the present model in PSHA will be conservative at the long return periods often used in engineering design.

Smoothed values of τ, σ, e_1, and e_3 are plotted in Figure 9. While both τ and σ are period-dependent, the period-dependence of σ_v is dependent on site condition.

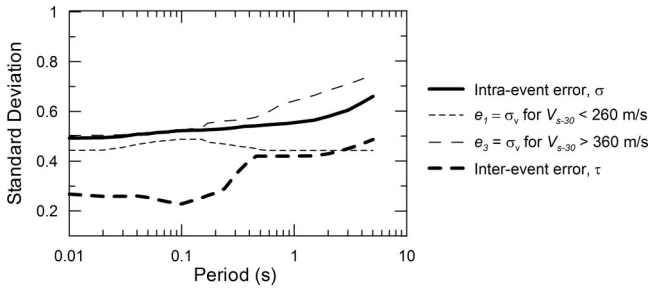

Figure 9. Variation of standard deviation terms with period (Model A1) showing strong period dependence of σ for relatively stiff soils, but weak dependence for softer soils.

We find no significant period-dependence for relatively soft soils (i.e., e_1 in Figure 9, $V_{s\text{-}30}<260$ m/s), but strong dependence for stiffer materials (e_3, $V_{s\text{-}30}>360$ m/s).

COMPARISONS TO PREVIOUS STUDIES

VELOCITY-DEPENDENCE OF AMPLIFICATION

The Model A1–A3 regression results from Equation 5 are plotted for $PHA_r=0.1$ g in Figure 10, and are compared to the results of previous studies discussed above. Parameters c and V_{ref} are also compared to those from previous studies in Table 4. The slope values c are seen to be comparable to those from previous studies (except Steidl). However, the V_{ref} values for Models A1–A3 are significantly smaller than those from

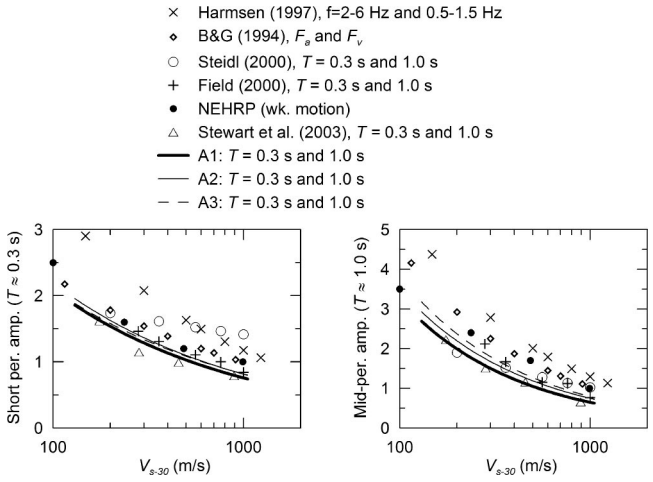

Figure 10. Comparison of $V_{s\text{-}30}$ dependence of $F(0.3)$ and $F(1.0)$ parameters (evaluated at $PHA_r=0.1$ g) from this study to short- and mid-period amplification functions from previous studies.

Table 4. Comparison of power law slope (c) and reference velocity (V_{ref}) parameters from this study (unsmoothed) to those from previous work

Parameter		This Study A1[1]	This Study A2[1]	This Study A3[1]	B & G (1994)[2]	Harmsen (1997)[3]	Field (2000)[4]	Steidl (2000)[5]
c	$F(0.3)$	−0.46±0.07	−0.44±0.07	−0.44±0.07	−0.36	−0.56	−0.35	−0.13
	$F(1.0)$	−0.69±0.07	−0.66±0.08	−0.67±0.07	−0.64	−0.66	−0.70	−0.39
V_{ref} (m/s)	$F(0.3)$	532±93	601±103	610±106	997	1370	760	—
	$F(1.0)$	519±69	646±90	709±107	1067	1140	760	1054

[1] results of present study—before smoothing
[2] results for period range T=0.1–0.5 s in $F(0.3)$ row, results for T=0.4–2.0 s shown in $F(1.0)$ row
[3] results for period range T=0.17–0.5 s in $F(0.3)$ row, results for T=0.7–2.0 s shown in $F(1.0)$ row
[4] value of V_{ref} preselected as 760 m/s and other regression parameters adjusted accordingly
[5] results for data with PHA<0.1g; — = parameter not established

other studies, which reflects the relatively soft reference site condition associated with the attenuation relationships used here to develop reference motions. However, our V_{ref} values are generally similar to the $V_{s\text{-}30}$ values compiled by Silva et al. (1997) (median =520 m/s) and Boore et al. (1997) (average=620 m/s) from boreholes at rock sites in active regions.

AMPLIFICATION LEVELS WITHIN NEHRP CATEGORIES

In this section we seek to compare the amplification factors within NEHRP categories predicted by Models A1–A3 with those utilized within the *NEHRP Provisions* (BSSC 2001) and those identified by previous investigators. It is necessary to first remove the bias associated with inconsistent reference site conditions before such comparisons can be made.

The regression model in Equation 5 enables insight to be developed into the bias associated with the use of a rock-average site condition (in active regions) to represent the intended NEHRP reference condition of $V_{s\text{-}30}$=760 m/s. This bias can be calculated as follows:

$$\ln B(T) = c \cdot \ln\left(\frac{V_{ref}}{760}\right) \tag{8}$$

where $B(T)$ indicates bias at period T. Equation 8 strictly holds only when nonlinearity parameter b is the same for velocities of V_{ref} and 760 m/s. While that is generally not exactly true (due to the linear taper in b indicated by Equation 3d), Equation 8 nonetheless provides a good approximation of bias because of small nonlinearity at these high velocities. At T=0.3 and 1.0 s, the resulting biases for Models A1–A3 are approximately 1.09–1.17 and 1.05–1.28, respectively.

The $B(T)$ values are combined with the A1–A3 amplification models to enable comparisons to the site factors in the *NEHRP Provisions* for a consistent reference site condition of $V_{s\text{-}30}$=760 m/s. Plotted in Figure 11 are the NEHRP factors along with the average of bias-adjusted predictions of amplification Models A1–A3 over a range of $V_{s\text{-}30}$

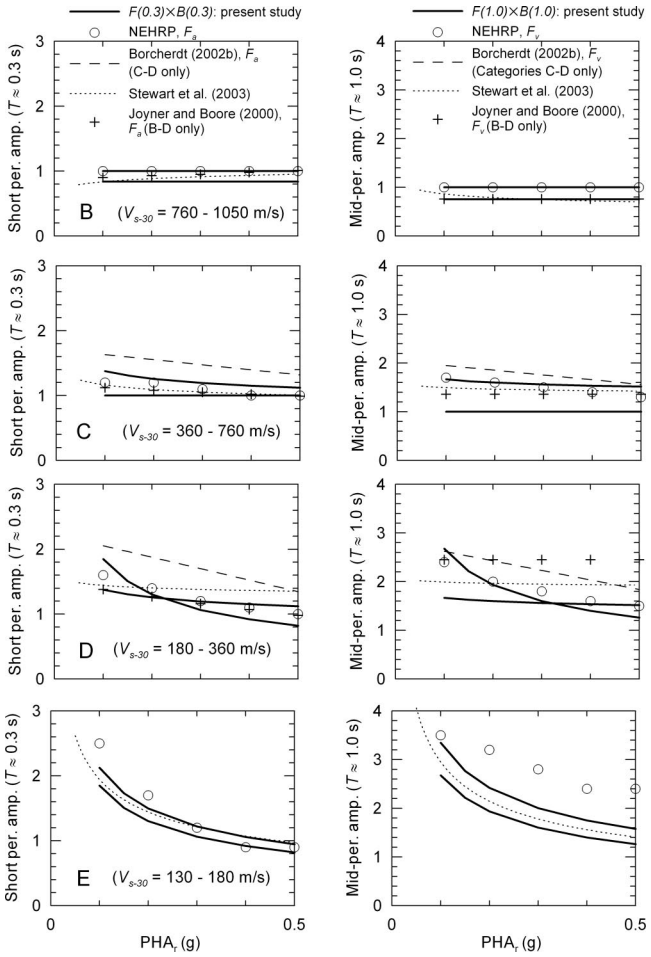

Figure 11. Comparison of bias-adjusted average amplification factors (reference site condition of $V_{s\text{-}30}$=760 m/s) from Models A1–A3 for the indicated velocity ranges to amplification factors by others, including (1) NEHRP (intended to apply for a reference site condition of $V_{s\text{-}30}$=760 m/s); (2) Borcherdt (2002b) (reference condition of approximately 850 m/s); (3) Stewart et al. (2003) factors bias-adjusted (using Equation 8) to reference condition of $V_{s\text{-}30}$=760 m/s; and (4) Joyner and Boore (2000) for reference condition of $V_{s\text{-}30}$=760 m/s.

appropriate to the respective categories. In the averaging across Models A1–A3, equal weight was given to each model. The variability between the models in this case is smaller than that shown in Figure 6 because of the bias removal, which adjusts all of the models to a common reference velocity of 760 m/s. Also shown in Figure 11 are (1) the Borcherdt (2002b) amplification factors, which apply for a slightly stiffer reference site condition of $V_{s\text{-}30}$=850 m/s; (2) the amplification factors for NEHRP categories by

Stewart et al. (2003), which have been adjusted to a reference site condition of 760 m/s using the bias adjustment factor in Equation 8; and (3) the Joyner and Boore (2000) amplification factors for reference condition $V_{s\text{-}30}$=760 m/s.

The bias-adjusted average amplification factors from this study are often smaller than those given in the *NEHRP Provisions*. In the case of Categories B-D, the upper-bound bias-adjusted factors from this study are similar to the NEHRP factors. The nonlinearity represented by the NEHRP factors for Categories B-E is generally similar to that for our factors. In the case of Category D, the NEHRP nonlinearity appears to coincide with the mid-range nonlinearity from the present study. For Category E, the bias-adjusted factors from this study are generally comparable to NEHRP at small period, but are considerably smaller than NEHRP for mid-periods.

The offset between our bias-adjusted factors and the NEHRP factors warrants further discussion. At issue here is whether the NEHRP factors are conservatively biased. One possible explanation for the discrepancy is that the NEHRP factors, as presently formulated, apply for a site condition stiffer than the intended target of 760 m/s. Recall that the empirical basis for the NEHRP factors is observations from the 1989 Loma Prieta earthquake (corresponding to $PHA_r \approx 0.1$ g). As reported by Borcherdt and Glassmoyer (1994), the velocity at which the amplification function derived from those data is unity is approximately 1000 m/s. This velocity is contradicted somewhat by Borcherdt (2002b), who reports that the average velocity at those sites based on borehole measurements is 795 m/s. Nonetheless, the regressed site amplification model used in the original development of the NEHRP site factors is unity near 1000 m/s, so that is the more relevant velocity to the present discussion. Thus, the existing NEHRP factors are likely biased for their intended reference site condition of 760 m/s by amounts on the order of ~12% for F_a and ~20% for F_v (based on Equation 8). Accordingly, it appears that a significant portion of the discrepancies observed in Figure 11 can be explained by apparent bias in the present NEHRP factors.

The amplification factors from Borcherdt (2002b) are generally larger than the NEHRP factors and the results of this study. This may be due in part to the stiffer reference site condition of $V_{s\text{-}30}$=850 m/s. The amplification factors from Stewart et al. (2003) either fall near the middle of the range of velocity-dependent factors from this study (e.g., C, E), or are near the middle of the range at low PHA_r but have less nonlinearity and, hence, higher amplification at high PHA_r (e.g., D). The amplification factors by Joyner and Boore are generally consistent with the results of the present study except for long period amplification for Category D.

STANDARD DEVIATION TERMS

Figure 12 shows the standard deviation terms calculated in this study along with those proposed in the various attenuation relationships used here. The top frame compares Model A1 standard deviation terms to those from the A&S attenuation relationship. The inter- and intra-event standard deviation terms are plotted separately, and the intra-event terms are separated by site condition. Note that the A&S terms are magnitude dependent.The standard deviation terms from this study are generally consistent with A&S, except that Model A1 τ is period dependent, and exceeds the A&S τ for

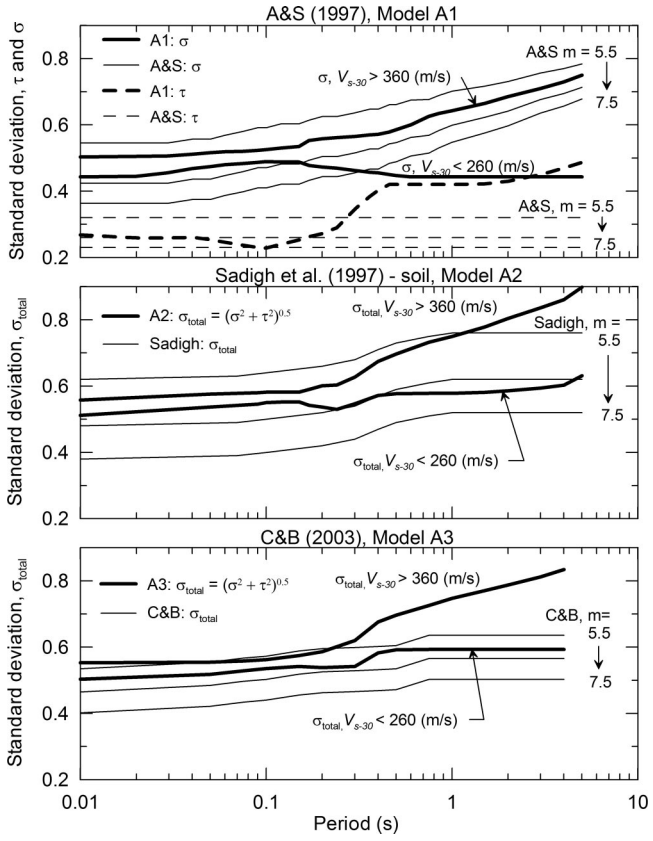

Figure 12. Comparison of error terms from this study to those from attenuation models.

$T>0.3$ s. The middle frame is based on Model A2 and Sadigh et al. (1997) soil attenuation, and shows only the total standard deviation (σ_{total}). The standard deviation from Model A2 is generally similar to the Sadigh results for soil. The bottom frame is based on Model A3 and C&B (Campbell and Bozorgnia 2003) attenuation, and again shows total standard deviation (σ_{total}). The Model A3 standard deviation terms for stiff soils/rock are larger than the C&B terms, whereas the Model A3 results for relatively soft soils is consistent with the C&B results.

EFFECTIVENESS OF V_{S-30} AS SITE CONDITION METRIC

Stewart et al. (2003) investigated the relative effectiveness of several classification schemes for use in strong motion prediction by evaluating an intra-event standard deviation term that represents the average prediction dispersion across all categories in each scheme. Since the standard deviation terms were calculated across all categories, they were denoted "intercategory standard deviation (σ_R)."

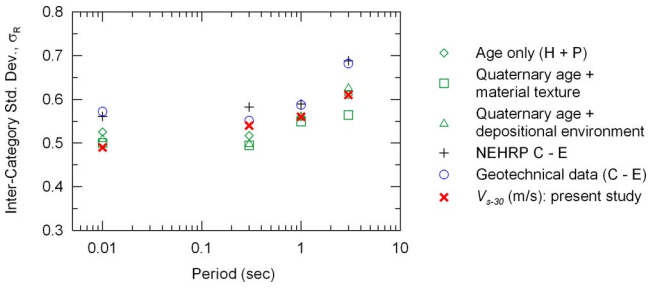

Figure 13. Intercategory standard deviation terms for spectral acceleration, soil categories.

A scheme is considered to be relatively effective at capturing site-to-site variations in ground motion when σ_R is small, and is less effective when σ_R is large. As shown in Figure 13, it was found that detailed surface geology based classification schemes are more effective than NEHRP categories (i.e., Table 1) or a geotechnical scheme (Rodriguez-Marek et al. 2001). In Figure 13, the intra-event standard deviation from this study is compared to those found by Stewart et al. (2003). The relatively low standard deviations from this study indicate that with the model proposed herein, the $V_{s\text{-}30}$ site metric is more effective than NEHRP or geotechnical classification schemes at most periods, and roughly equally effective as detailed surface geology.

CONCLUSIONS AND RECOMMENDATIONS

In this paper, we have developed a model for ground motion amplification that is a function of $V_{s\text{-}30}$ and PHA_r. The amplification factors are defined relative to "rock" reference motions from several attenuation relationships for active tectonic regions, including those of Abrahamson and Silva (1997), Sadigh et al. (1997), and Campbell and Bozorgnia (2003). Amplification at short- and mid-period ranges was shown to decrease with increasing velocity in a manner similar to trends identified in previous studies. The nonlinearity of amplification factors was found to vary with $V_{s\text{-}30}$, being significant for $V_{s\text{-}30}<180$ m/s and relatively small for $V_{s\text{-}30}>300$ m/s. Standard deviation terms were found to have a significant dependence on $V_{s\text{-}30}$. The databases used in model development cover the parameter spaces $V_{s\text{-}30}=130-1300$ m/s and $PHA_r=0.02-0.8$ g, and the model is only considered valid across that range of parameters.

The model resulting from this work can be used as a site term in empirical attenuation relations, and could be utilized to parameterize site effects in the future development of attenuation relationships. The model is applied by using Equation 5 with $V_{s\text{-}30}$ defined from site characterization, PHA_r defined for reference rock conditions using one of the attenuation relationships used here, and b defined per Equation 3. Model parameters can be taken from the Appendix for the corresponding attenuation models (i.e., A1—A&S; A2—Sadigh et al.; A3—C&B). For modeling ground motions during a future earthquake, event term η in Equation 5 is generally taken as zero for calculation of the median. The corresponding error term can be taken as σ_{total} from the Appendix, or

for a more accurate assessment, can be evaluated using Equation 6 with τ taken from the Appendix and σ calculated using the site-dependent model in Equation 7 (in which case, σ is denoted σ_v).

The results of this work provide insight into the accuracy of the site coefficients in the existing *NEHRP Provisions* and *Commentary* (BSSC 2001). Several important implications of this work are as follows:

1. We utilized an entirely different procedure for evaluating amplification factors than that employed in the development of the current NEHRP recommendations (described in Dobry et al., 2000). In many cases, there are significant discrepancies between our factors and those in the *NEHRP Provisions*, with our site factors often being lower. These new results warrant consideration for future versions of the *NEHRP Provisions* and *Commentary*.
2. The standard deviation analysis results provide evidence for $V_{s\text{-}30}$-dependence of intra-event dispersion (σ). For relatively soft materials, σ has no significant period dependency and is relatively low. For stiffer materials, σ is strongly period-dependent such that the offset from the soft soil values is small at low periods but reaches values up to 0.3 at long period. This result suggests a potential for bias in the procedure by which spectral ordinates are evaluated in the *NEHRP Provisions*. In that procedure, design spectral ordinates are calculated as the product of PSHA results and amplification factors. The bias would arise when the dispersion values used in the attenuation relationship for PSHA are different from what is appropriate for the site category.
3. The development of national hazard maps appropriate for the reference site condition of $V_{s\text{-}30}=760$ m/s requires the correction of existing attenuation models, because the databases used in the development of these models do not share the NEHRP reference site condition. The correction factors for the various attenuation models can be evaluated using Equation 8 and the coefficients tabulated in the Appendix.

ACKNOWLEDGMENTS

Support for this study was provided by the Pacific Earthquake Engineering Research Center through the Earthquake Engineering Research Centers Program of the National Science Foundation under Award Number EEC-9701568. Rie Von Eyben, Xiao Chen, Philip Ender, and Steve Erickson provided valuable consultation regarding the statistical analyses. We would also like to thank Kenneth Campbell for his assistance in compiling distance parameters for strong motions stations. We thank Dr. Campbell and Dr. Ned Field, along with two anonymous reviewers, for providing helpful review comments.

APPENDIX

Tables A1–A3 show the model parameters for the corresponding attenuation models: Model A1 for A&S (Abrahamson and Silva 1997), Model A2 for Sadigh et al. (1997), and Model A3 for C&B (Campbell and Bozorgnia 2003).

Table A1. Smoothed model parameters for Model A1

Period (sec)	b_1	V_{ref} (m/sec)	c	b_2	τ	σ	e_1	e_3
0.01	−0.64	418±72	−0.36±0.06	−0.14±0.04	0.27	0.49	0.44	0.50
0.02	−0.63	490±101	−0.34±0.06	−0.12±0.04	0.26	0.50	0.45	0.51
0.03	−0.62	324±58	−0.33±0.06	−0.11±0.04	0.26	0.50	0.46	0.51
0.04	−0.61	233±49	−0.31±0.06	−0.11±0.04	0.26	0.51	0.47	0.51
0.05	−0.64	192±48	−0.29±0.06	−0.11±0.04	0.25	0.51	0.47	0.52
0.06	−0.64	181±53	−0.25±0.06	−0.11±0.04	0.25	0.52	0.48	0.52
0.075	−0.64	196±57	−0.23±0.06	−0.11±0.04	0.24	0.52	0.48	0.52
0.09	−0.64	239±64	−0.23±0.07	−0.12±0.04	0.23	0.52	0.49	0.52
0.10	−0.60	257±61	−0.25±0.07	−0.13±0.04	0.23	0.52	0.49	0.53
0.12	−0.56	299±66	−0.26±0.07	−0.14±0.04	0.24	0.52	0.49	0.53
0.15	−0.53	357±83	−0.28±0.07	−0.18±0.04	0.25	0.53	0.49	0.54
0.17	−0.53	406±86	−0.29±0.07	−0.19±0.04	0.26	0.53	0.48	0.55
0.20	−0.52	453±97	−0.31±0.07	−0.19±0.04	0.27	0.53	0.47	0.56
0.24	−0.52	493±91	−0.38±0.07	−0.16±0.04	0.29	0.53	0.47	0.56
0.30	−0.52	532±93	−0.44±0.07	−0.14±0.05	0.35	0.54	0.46	0.57
0.36	−0.51	535±97	−0.48±0.07	−0.11±0.05	0.38	0.54	0.46	0.57
0.40	−0.51	535±104	−0.50±0.07	−0.10±0.05	0.40	0.54	0.46	0.57
0.46	−0.50	535±87	−0.55±0.07	−0.08±0.05	0.42	0.54	0.45	0.58
0.50	−0.50	535±82	−0.60±0.07	−0.06±0.05	0.42	0.54	0.45	0.59
0.60	−0.49	535±73	−0.66±0.07	−0.03±0.05	0.42	0.55	0.44	0.60
0.75	−0.47	535±75	−0.69±0.07	0.00±0.05	0.42	0.55	0.44	0.63
0.85	−0.46	535±73	−0.69±0.07	0.00±0.05	0.42	0.55	0.44	0.63
1.00	−0.44	535±69	−0.70±0.07	0.00±0.05	0.42	0.56	0.44	0.64
1.50	−0.40	535±63	−0.72±0.08	0.00±0.06	0.42	0.57	0.44	0.67
2.00	−0.38	535±61	−0.73±0.08	0.00±0.06	0.43	0.58	0.44	0.69
3.00	−0.34	535±65	−0.74±0.09	0.00±0.07	0.45	0.61	0.44	0.71
4.00	−0.31	535±110	−0.75±0.09	0.00±0.07	0.47	0.64	0.44	0.73
5.00	−0.30	535±166	−0.75±0.14	0.00±0.11	0.49	0.66	0.44	0.75

Table A2. Smoothed model parameters for Model A2

Period (sec)	b_1	V_{ref} (m/sec)	c	b_2	τ	σ	e_1	e_3
0.01	−0.61	567±110	−0.34±0.06	−0.20±0.04	0.24	0.49	0.45	0.51
0.05	−0.66	521±128	−0.26±0.06	−0.25±0.04	0.24	0.52	0.48	0.52
0.09	−0.62	497±147	−0.21±0.07	−0.24±0.04	0.24	0.52	0.49	0.53
0.10	−0.58	464±122	−0.22±0.07	−0.24±0.04	0.24	0.52	0.50	0.53
0.12	−0.53	444±109	−0.24±0.06	−0.24±0.04	0.24	0.52	0.50	0.53
0.15	−0.51	508±134	−0.25±0.06	−0.24±0.04	0.24	0.52	0.50	0.53
0.17	−0.50	545±128	−0.26±0.06	−0.24±0.04	0.24	0.52	0.49	0.54
0.20	−0.50	580±142	−0.29±0.06	−0.23±0.04	0.24	0.52	0.48	0.55
0.24	−0.50	600±119	−0.36±0.07	−0.23±0.04	0.25	0.52	0.47	0.55
0.30	−0.49	620±103	−0.43±0.07	−0.22±0.04	0.29	0.53	0.47	0.56
0.40	−0.49	640±119	−0.50±0.07	−0.21±0.04	0.34	0.54	0.46	0.58
0.50	−0.49	640±99	−0.55±0.07	−0.19±0.04	0.35	0.55	0.46	0.60
0.75	−0.48	645±99	−0.63±0.08	−0.15±0.05	0.36	0.56	0.46	0.64
1.00	−0.48	646±90	−0.67±0.08	−0.15±0.05	0.36	0.57	0.46	0.66
1.50	−0.47	640±85	−0.70±0.08	−0.14±0.05	0.36	0.58	0.46	0.69
2.00	−0.46	580±75	−0.72±0.08	−0.14±0.05	0.37	0.59	0.46	0.72
3.00	−0.43	545±68	−0.72±0.10	−0.14±0.07	0.38	0.62	0.46	0.75
4.00	−0.40	540±121	−0.72±0.10	−0.13±0.07	0.39	0.65	0.46	0.77
5.00	−0.39	535±130	−0.72±0.14	−0.13±0.11	0.44	0.68	0.46	0.79

Table A3. Smoothed model parameters for Model A3

Period (sec)	b_1	V_{ref} (m/sec)	c	b_2	τ	σ	e_1	e_3
0.01	−0.55	501±90	−0.34±0.06	−0.04±0.05	0.23	0.49	0.45	0.50
0.05	−0.57	676±179	−0.26±0.06	−0.05±0.05	0.21	0.51	0.47	0.51
0.075	−0.61	780±280	−0.21±0.06	−0.11±0.05	0.22	0.51	0.48	0.52
0.10	−0.57	643±198	−0.22±0.07	−0.12±0.05	0.22	0.51	0.49	0.52
0.15	−0.52	541±142	−0.24±0.06	−0.13±0.05	0.23	0.52	0.49	0.53
0.20	−0.51	565±129	−0.28±0.06	−0.07±0.05	0.25	0.52	0.48	0.53
0.30	−0.51	610±106	−0.41±0.07	−0.04±0.05	0.29	0.53	0.46	0.55
0.40	−0.50	640±134	−0.50±0.07	−0.02±0.05	0.37	0.54	0.45	0.57
0.50	−0.50	660±102	−0.59±0.07	−0.02±0.05	0.39	0.54	0.45	0.58
0.75	−0.49	703±101	−0.65±0.07	−0.02±0.06	0.39	0.55	0.45	0.62
1.00	−0.49	709±107	−0.68±0.07	−0.04±0.06	0.39	0.56	0.45	0.64
1.50	−0.48	710±117	−0.71±0.08	−0.12±0.06	0.39	0.57	0.45	0.67
2.00	−0.46	710±113	−0.72±0.08	−0.17±0.06	0.39	0.58	0.45	0.69
3.00	−0.42	710±87	−0.72±0.09	−0.22±0.08	0.39	0.61	0.45	0.72
4.00	−0.40	710±161	−0.72±0.10	−0.25±0.08	0.39	0.63	0.45	0.74

REFERENCES

Abrahamson, N. A., 2000. Effects of rupture directivity on probabilistic seismic hazard analysis, *Proceedings of 6th International Conference on Seismic Zonation, November 12–15, Palm Springs, CA*, Earthquake Engineering Research Institute, Oakland, CA.

Abrahamson, N. A., and Silva, W. J., 1997. Empirical response spectral attenuation relations for shallow crustal earthquakes, *Seismol. Res. Lett.* **68**, 94–127.

Abrahamson, N. A., and Youngs, R. R., 1992. A stable algorithm for regression analyses using the random effects model, *Bull. Seismol. Soc. Am.* **82**, 505–510.

Anderson, J. G., Trifunac, M. D., Teng, T.-L., Amini, A., and Moslem, K., 1981. Los Angeles vicinity strong motion accelerograph network, *Report No. CE 81-04*, Univ. of Southern California.

Baturay, M. B., and Stewart, J. P., 2003. Uncertainty and bias in ground motion estimates from ground response analyses, *Bull. Seismol. Soc. Am.* **93**, 2025–2042.

Bazzuro, P., 1998. Probabilistic Seismic Demand Analysis, Ph.D. dissertation, Civil Engineering Dept., Stanford University.

Boore, D. M., Joyner, W. B., and Fumal, T. E., 1997. Equations for estimating horizontal response spectra and peak acceleration from western North American earthquakes: A summary of recent work, *Seismol. Res. Lett.* **68**, 128–153.

Boore, D. M., and Brown, L. T., 1998. Comparing shear wave velocity profiles from inversion of surface wave phase velocities with downhole measurements: Systematic differences between the CXW method and down hole measurements at six USC strong motion sites, *Seismol. Res. Lett.* **69**, 222–229.

Borcherdt, R. D., 1994. Estimates of site-dependent response spectra for design (methodology and justification), *Earthquake Spectra* **10** (4), 617–653.

Borcherdt, R. D., 2002a. Empirical evidence for acceleration-dependent amplification factors, *Bull. Seismol. Soc. Am.* **92**, 761–782.

Borcherdt, R. D., 2002b. Empirical evidence for site coefficients in building code provisions, *Earthquake Spectra* **18** (2), 189–217.

Borcherdt, R. D., and Glassmoyer, G., 1994. Influences of local geology on strong and weak ground motions recorded in the San Francisco Bay region and their implications for site-specific building-code provisions, *The Loma Prieta, California Earthquake of October 17, 1989—Strong Ground Motion, U.S. Geological Survey Professional Paper 1551-A*, A77-A108

Building Seismic Safety Council (BSSC), 2001. *NEHRP Recommended Provisions for Seismic Regulations for New Buildings and Other Structures, Part 1: Provisions* and *Part 2: Commentary*, Federal Emergency Management Agency, *FEMA-368* and *FEMA-369*, Washington D.C., February.

Campbell, K. W., and Bozorgnia, Y., 2003. Updated near-source ground-motion (attenuation) relations for the horizontal and vertical components of peak ground acceleration and acceleration response spectra, *Bull. Seismol. Soc. Am.* **93**, 314–331.

Dobry, R., Martin, G. R., Parra, E., and Bhattacharyya, A., 1994. Development of site-dependent ratios of elastic response spectra (RRS) and site categories for building seismic codes, *Proceedings of 1992 NCEER/SEAOC/BSSC Workshop on Site Response During Earthquakes and Seismic Code Provisions*, edited by G. R. Martin, University of Southern California, National Center for Earthquake Engineering Research Special Publication *NCEER-94-SP01*, Buffalo, NY.

Dobry, R., Borcherdt, R. D., Crouse, C. B., Idriss, I. M., Joyner, W. B., Martin, G. R., Power, M. S., Rinne, E. E., and Seed, R. B., 2000. New site coefficients and site classification system used in recent building seismic code provisions, *Earthquake Spectra* **16** (1), 41–67.

Field, E. H., 2000. A modified ground motion attenuation relationship for southern California that accounts for detailed site classification and a basin depth effect, *Bull. Seismol. Soc. Am.* **90**, S209–S221.

Frankel, A., Mueller, C., Barnhard, T., Leyendecker, E., Wesson, R., Harmsen, A., Klein, F., Perkins, D., Dickman, N., Hanson, S., and Hopper, M., 2000. USGS national seismic hazard maps, *Earthquake Spectra* **16** (1), 1–20.

Harmsen, S. C., 1997. Determination of site amplification in the Los Angeles urban area from inversion of strong motion records, *Bull. Seismol. Soc. Am.* **87**, 866–887.

Joyner, W. B., and Boore, D. M., 2000. Recent developments in earthquake ground motion estimation, *Proceedings of 6th International Conference on Seismic Zonation, November 12–15, Palm Springs, CA*, Earthquake Engineering Research Institute, Oakland, CA.

Joyner, W. B., Fumal, T. E., and Glassmoyer, G., 1994. Empirical response spectral ratios for strong motion data from the 1989 Loma Prieta, California, earthquake, *Proceedings of 1992 NCEER/SEAOC/BSSC Workshop on Site Response During Earthquakes and Seismic Code Provisions*, edited by G. R. Martin, University of Southern California, National Center for Earthquake Engineering Research Special Publication *NCEER-94-SP01*, Buffalo, NY.

Leyendecker, E. V., Hunt, R. J., Frankel, A. D., and Rukstales, K. S., 2000. Development of maximum considered earthquake ground motion maps, *Earthquake Spectra* **16** (1), 21–40.

Pinheiro, J. C., and Bates, D. M., 2000. *Mixed-Effects Models in S and S-PLUS*, Springer, New York.

Raudenbush, S. W., and Bryk, A. S., 2002. *Hierarchical Linear Models: Applications and Data Analysis Methods*, 2nd Edition, Sage Publications, Thousand Oaks, CA.

Rodriguez-Marek, A., Bray, J. D., and Abrahamson, N. A., 2001. An empirical geotechnical seismic site response procedure, *Earthquake Spectra* **17** (1), 65–87.

Rodriguez-Ordonez, J. A., 1994. A New Method for Interpretation of Surface Wave Measurements in Soils, Ph.D. dissertation, North Carolina State University, Raleigh.

Sadigh, K., Chang, C.-Y., Abrahamson, N. A., Chiou, S. J., and Power, M. S., 1993. Specification of long-period ground motions: Updated attenuation relationships for rock site conditions and adjustment factors for near-fault effects, *Proceedings of Seminar on Seismic Isolation, Passive Energy Dissipation, and Active Control*, Applied Technology Council Publication No. 17-1, Vol. 1, pp. 59–70.

Sadigh, K., Chang, C.-Y., Egan, J. A., Makdisi, F., and Youngs, R. R., 1997. Attenuation relations for shallow crustal earthquakes based on California strong motion data, *Seismol. Res. Lett.* **68**, 180–189.

Seed, R. B., Dickenson, S. E., Rau, G. A., White, R. K., and Mok, C. M., 1994. Observations regarding seismic response analyses for soft and deep clay sites, *Proceedings of 1992 NCEER/SEAOC/BSSC Workshop on Site Response During Earthquakes and Seismic Code Provisions*, edited by G. R. Martin, University of Southern California, National Center for Earthquake Engineering Research Special Publication *NCEER-94-SP01*, Buffalo, NY.

Silva, W. J., Abrahamson, N., Toro, G., and Costantino, C., 1997. Description and validation of the stochastic ground motion model, report to Brookhaven National Laboratory, Associated Universities, Inc., Upton, NY, available at http://www.pacificengineering.org

Somerville, P. G., Smith, N. F., Graves, R. W., and Abrahamson, N. A., 1997. Modification of

empirical strong ground motion attenuation relations to include the amplitude and duration effects of rupture directivity, *Seismol. Res. Lett.* **68**, 199–222.

Steidl, J. H., 2000. Site response in southern California for probabilistic seismic hazard analysis, *Bull. Seismol. Soc. Am.* **90**, S149–S169.

Stewart, J. P., Liu, A. H., Choi, Y., and Baturay, M. B., 2001. Amplification factors for spectral acceleration in active regions, *Report No. PEER-2001/10*, Pacific Earthquake Engineering Research Center, University of California, Berkeley.

Stewart, J. P., Liu, A. H., and Choi, Y., 2003. Amplification factors for spectral acceleration in tectonically active regions, *Bull. Seismol. Soc. Am.* **93**, 332–352.

Wills, C. J., and Silva, W., 1998. Shear wave velocity characteristics of geologic units in California, *Earthquake Spectra* **14** (3), 533–556.

Youngs, R. R., 1993. Soil amplification and vertical to horizontal ratios for analysis of strong motion data from active tectonic regions, Appendix 2C in *Guidelines for Determining Design Basis Ground Motions*, Vol. 2, Electrical Power Research Institute, *Report No. TR-102293*.

Youngs, R. R., Abrahamson, N. A., Makdisi, F. I., and Sadigh, K., 1995. Magnitude-dependent variance of peak ground acceleration, *Bull. Seismol. Soc. Am.* **85**, 1161–1176.

(Received 22 September 2003; accepted 12 July 2004)